

Thiacyclophane Complexes of Rhodium and Iridium. Synthesis, Structure, and Reactivity of [M(COD)(L)][BF₄] (M = Rh, Ir; L = 2,5,8-Trithia[9]-*o*-cyclophane (TT[9]OC), 5-Oxa-2,8-dithia[9]-*o*-cyclophane (ODT[9]OC))

Hilary A. Jenkins and Stephen J. Loeb*

Department of Chemistry and Biochemistry, University of Windsor,
Windsor, Ontario, Canada N9B 3P4

Received December 10, 1993*

The complexes [M(COD)(L)][BF₄] (M = Rh, Ir; L = 2,5,8-trithia[9]-*o*-cyclophane (TT[9]OC), 5-oxa-2,8-dithia[9]-*o*-cyclophane (ODT[9]OC)) were prepared in acetone by the reaction of [MCl(COD)]₂ with 2 equiv each of AgBF₄ and L. [Rh(COD)(TT[9]OC)][BF₄] (1) crystallized in the space group *Pca*2₁ with *a* = 23.951(4) Å, *b* = 8.845(2) Å, *c* = 10.463(8) Å, *V* = 2217(1) Å³, and *Z* = 4. The structure was refined to *R* = 5.26% and *R_w* = 5.70% for 1192 reflections with *F_o*² > 3σ(*F_o*²). [Ir(COD)(TT[9]OC)][BF₄] (2) crystallized in space group *P* $\bar{1}$ with *a* = 11.085(6) Å, *b* = 12.649(2) Å, *c* = 7.965(2) Å, α = 103.10(1)°; β = 93.93(1)°; γ = 89.45(1)°, *V* = 1085.2(5) Å³, and *Z* = 2. The structure was refined to *R* = 4.06% and *R_w* = 4.41% for 2935 reflections with *F_o*² > 3σ(*F_o*²). 1 and 2 have trigonal bipyramidal geometry with the benzylic S atoms and an olefinic bond occupying the equatorial sites and the central S atom and the other olefinic bond in the axial positions. [Rh(COD)(ODT[9]OC)][BF₄] (3) crystallized in the space group *P*2₁/*c* with *a* = 9.173(2) Å, *b* = 24.173(6) Å, *c* = 9.907(3) Å, β = 94.14(3)°; *V* = 2190(2) Å³, and *Z* = 4. The structure refined to *R* = 5.84% and *R_w* = 6.87% for 2312 reflections with *F_o*² > 3σ(*F_o*²). [Ir(COD)(ODT[9]OC)][BF₄] (4) crystallized in the space group *P* $\bar{1}$ with *a* = 9.677(3) Å, *b* = 13.142(6) Å, *c* = 8.996(2) Å, α = 107.48(3)°; β = 92.87(3)°; γ = 97.46(3)°, *V* = 1077.2(7) Å³, and *Z* = 2. The structure was refined to *R* = 7.38% and *R_w* = 6.59% for 3802 reflections with *F_o*² > 3σ(*F_o*²). 3 and 4 are square planar complexes with the benzylic S atoms and olefinic bonds coordinated. Reaction of 1 with CO yielded the complexes [Rh(CO)₂(TT[9]OC)][BF₄] (5) and [(TT[9]OC)Rh(μ-CO)₃Rh(TT[9]OC)][BF₄]₂ (6). 2 was relatively unreactive toward CO; however, reactions with [IrCl(COE)]₂ yielded [Ir(COE)(CO)(TT[9]OC)][BF₄] (7) and [Ir(CO)₂(TT[9]OC)][BF₄] (8) upon reaction with TT[9]OC and CO. [Ir(COE)(CO)(TT[9]OC)][BF₄] (7) crystallized in the space group *Pbca* with *a* = 23.338(5) Å, *b* = 24.646(9) Å, *c* = 13.805(5) Å, *V* = 7940(4) Å³, and *Z* = 8. The structure was refined to *R* = 7.68% and *R_w* = 7.98% for 1493 reflections with *F_o*² > 3σ(*F_o*²). 7 has trigonal bipyramidal geometry similar to 2 with the CO group in an axial position. 3 and 4 reacted with CO to yield [Rh(CO)₃(ODT[9]OC)][BF₄] (9) and [Ir(CO)₃(ODT[9]OC)][BF₄] (10), respectively. Reactions of 1-4 with NOBF₄ yielded the adducts [M(NO)(COD)(L)][BF₄]₂ (11-14). [Ir(NO)(COD)(ODT[9]OC)][BF₄]₂ (14) crystallized in the space group *Pnma* with *a* = 18.821(6) Å, *b* = 9.611(5) Å, *c* = 14.225(8) Å, *V* = 2573(2) Å³, and *Z* = 4. The structure was refined to *R* = 5.11% and *R_w* = 4.83% for 1180 reflections with *F_o*² > 3σ(*F_o*²). 14 has square pyramidal geometry with the bent NO group in an apical position.

Introduction

The impressive reactivity of Rh and Ir complexes containing six-electron capping ligands such as tripodal phosphines, pyrazolylborates, and cyclopentadienyl ligands¹⁻³ has prompted initial investigations into the possibility of employing tridentate thioether macrocycles

such as 1,4,7-trithiacyclononane (9S3) as alternatives to these ancillary ligands.⁴ Schröder prepared and structurally characterized [Rh(R)(9S3)]⁺ and [Ir(R)(9S3)]⁺ (R = (ethylene)₂, 1,5-COD),⁵ and although the reaction chemistry of these compounds has yet to be investigated in any detail, like some other Rh complexes of crown thioethers which have been found to be good nucleophiles,^{5,6} [Rh(COD)(9S3)]⁺ undergoes oxidative addition with CH₂Cl₂. Hill and co-workers have prepared organometallic Ru(II) complexes of 9S3^{7,8} by reacting [Ru(CH=CHR)Cl(CS)(PPh₃)₂] (R = H, C₄H₉, C₆H₄Me-4) with the crown

* Abstract published in *Advance ACS Abstracts*, April 1, 1994.

(1) (a) Bianchini, C.; Meli, A.; Peruzzini, M.; Vizza, F.; Zanobini, F. *Coord. Chem. Rev.* 1992, 120, 193-208 and references therein. (b) Bianchini, C.; Farnetti, E.; Graziani, M.; Kaspar, J.; Vizza, F. *J. Am. Chem. Soc.* 1993, 115, 1753-1759. (c) Barbaro, P.; Bianchini, C.; Meli, A.; Peruzzini, M.; Vacca, A.; Vizza, F. *Organometallics* 1991, 10, 2227-2238.

(2) (a) Janowicz, A. H.; Bergman, R. G. *J. Am. Chem. Soc.* 1983, 105, 3929-3939. (b) Hoyano, J. K.; McMaster, A. D.; Graham, W. A. G. *J. Am. Chem. Soc.* 1983, 105, 7190-7191. (c) Jones, W. D.; Feher, F. J. *J. Am. Chem. Soc.* 1986, 108, 4856-4867. (d) Jones, W. D.; Feher, F. J. *Acc. Chem. Res.* 1989, 22, 91-100 and references therein.

(3) (a) Ghosh, C. K.; Graham, W. A. G. *J. Am. Chem. Soc.* 1987, 109, 4726-4727. (b) Ghosh, C. K.; Graham, W. A. G. *J. Am. Chem. Soc.* 1989, 111, 375-376. (c) Jones, W. D.; Hessel, E. T. J. *J. Am. Chem. Soc.* 1992, 114, 6087-6095.

(4) (a) Copper, S. R. *Acc. Chem. Res.* 1988, 21, 141-146. (b) Blake, A. J.; Schröder, M. *Adv. Inorg. Chem.* 1990, 35, 1-80. (c) Cooper, S. R.; Rawle, S. C. *Struct. Bonding* 1990, 72, 1-72.

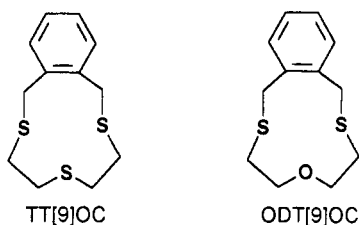
(5) Blake, A. J.; Halcrow, M. A.; Schröder, M. *J. Chem. Soc., Chem. Commun.* 1991, 253-256.

(6) Yoshida, T.; Ueda, T.; Adachi, T.; Yamamoto, K.; Higuchi, T. *J. Chem. Soc. Chem. Commun.* 1985, 1137-1138.

(7) Hill, A. F.; Alcock, N. W.; Cannadine, J. C.; Clark, G. R. *J. Organomet. Chem.* 1988, 356, 389-396.

thioether and have found that the "noninnocent" σ -(*E*)-vinyl ligands undergo migratory insertion with CS. In addition, Bennett⁹ recently showed that $[\text{Ru}(\eta^6\text{-C}_6\text{Me}_6)(9\text{S}3)]^{2+}$ reacts with KO^tBu to give the half-sandwich ruthenium(II) arene complex $[\text{Ru}(\text{SCH}=\text{CH}_2)(\eta^6\text{-C}_6\text{Me}_5\text{-CH}_2\text{CH}_2\text{CH}_2\text{SCH}_2\text{CH}_2\text{S})]$. Similarly, the reaction of $[\text{M}(9\text{S}3)_2]^{3+}$ ($\text{M} = \text{Co}, \text{Rh}, \text{Ir}$) with base leads to deprotonation at a methylene carbon and subsequent rearrangement of the carbanion to yield a vinyl thioether complex via C—S bond cleavage.¹⁰ In related work, we¹¹ and others¹² have shown that C—H activation of a macrocyclic thioether can lead to anionic, metalated ligands containing thioether donor atoms.

In our work on thiacyclophanes, we have shown that the ligand 2,5,8-trithia[9]-*o*-cyclophane (TT[9]OC) prefers to adopt a facial S_3 -coordination mode^{13–15} but can also form stable metal complexes involving only one or two of the S donor atoms.¹⁶ The related ligand 5-oxa-2,8-dithia-



[9]-*o*-cyclophane (ODT[9]OC) also has the potential for facial coordination, although the much poorer donor ability of the ether O atom may result in only the two S atoms participating in coordination. The small macrocyclic ring in these two ligands makes them ideal as capping ligands analogous to 9S3. However, the increased flexibility of the thiacyclophanes may allow for a wider variety of attainable structures in solution, resulting in the generation of unsaturated species and an enhanced reaction chemistry. We report herein the synthesis, structures, and basic reaction chemistry of the complexes $[\text{M}(\text{COD})(\text{L})]^+$, where $\text{M} = \text{Rh}, \text{Ir}$, COD = 1,5-cyclooctadiene, and $\text{L} = \text{TT}[9]\text{-OC}, \text{ODT}[9]\text{OC}$.

Experimental Section

$[\text{RhCl}(\text{COD})_2]$,¹⁷ $[\text{IrCl}(\text{COD})_2]$,¹⁸ $[\text{IrCl}(\text{COE})_2]$,¹⁹ and TT[9]-OC¹⁴ were prepared by literature methods. AgBF_4 , NOBF_4 , 3-oxapentane-1,5-dithiol, 3-thiapentane-1,5-dithiol, α, α' -dibromo-*o*-xylene, and all deuterated solvents were purchased from Aldrich

(8) Cannadine, J.; Hector, A.; Hill, A. F. *Organometallics* **1992**, *11*, 2323–2324.

(9) Bennett, M. A.; Goh, L. Y.; Willis, A. C. *J. Chem. Soc., Chem. Commun.* **1992**, 1180–1181.

(10) Blake, A. J.; Holder, A. J.; Hyde, T. I.; Küppers, H. J.; Schröder, M.; Stotzel, S.; Wieghardt, K. *J. Chem. Soc., Chem. Commun.* **1992**, 1600–1602.

(11) (a) Hanan, G. S.; Kickham, J. E. *Organometallics* **1992**, *11*, 3063–3068. (b) Giesbrecht, G. R.; Hanan, G. S.; Kickham, J. E.; Loeb, S. J. *Inorg. Chem.* **1992**, *31*, 3286–3290. (c) Kickham, J. E.; Loeb, S. J.; Murphy, S. L. *J. Am. Chem. Soc.* **1993**, *115*, 7031–7032. (d) Loeb, S. J.; Shimizu, G. K. H. *J. Chem. Soc., Chem. Commun.* **1993**, 1395–1397.

(12) Hanton, L. R.; Kemmitt, T. *J. Chem. Soc., Chem. Commun.* **1991**, 700–702.

(13) de Groot, B.; Loeb, S. J. *Inorg. Chem.* **1990**, *29*, 4084–4090.

(14) de Groot, B.; Giesbrecht, G. R.; Loeb, S. J.; Shimizu, G. K. H. *Inorg. Chem.* **1991**, *30*, 177–182.

(15) de Groot, B.; Hanan, G. S.; Loeb, S. J. *Inorg. Chem.* **1991**, *30*, 4644–4647.

(16) de Groot, B.; Jenkins, H. A.; Loeb, S. J. *Inorg. Chem.* **1992**, *31*, 203–208.

(17) Giordano, G. *Inorg. Synth.* **1979**, *19*, 218–220.

(18) Uson, R.; Oro, L. A.; Cabeza, J. A. *Inorg. Synth.* **1985**, *23*, 126–128.

(19) van der Ent, A.; Onderdelinden, A. L. *Inorg. Synth.* **1974**, *14*, 94–95.

and used as received. All reactions were carried out under an atmosphere of $\text{N}_2(\text{g})$ using standard Schlenk techniques, and all solvents were degassed prior to use. ^1H and $^{13}\text{C}\{^1\text{H}\}$ NMR spectra (300–220 K) were recorded at 300.1 and 75.4 MHz, respectively, on a Bruker AC300 spectrometer locked to the deuterated solvent. Infrared spectra were recorded on a Nicolet 5DX FTIR spectrometer. Elemental analyses were performed by Microanalytical Services, Delta, British Columbia, Canada.

Preparation of 5-Oxa-2,8-dithia[9]-*o*-cyclophane (ODT[9]OC). Cesium carbonate (11.58 g, 60 mmol) was suspended in DMF (600 mL) under an atmosphere of N_2 . To this mixture was added a solution of α, α' -dibromo-*o*-xylene (7.92 g, 30 mmol) and 3-oxapentane-1,5-dithiol (4.38 g, 30 mmol) in DMF (150 mL). The temperature of the reaction was maintained at 70 °C. After addition, the mixture was cooled to room temperature and stirred for a further 12 h. The DMF was removed under vacuum and the resulting solid residue extracted with CH_2Cl_2 (200 mL). The CH_2Cl_2 fraction was extracted with 0.05 M NaOH (2×125 mL) and then dried over anhydrous Na_2SO_4 . After filtration and removal of the solvent, the solid residue was recrystallized from anhydrous ethanol. Yield: 5.8 g (80%). $^{13}\text{C}\{^1\text{H}\}$ NMR (CDCl_3): δ 137.17, 130.79, 127.59 (aromatic), 72.20 (OCH_2), 33.97 (benzylic), 32.57 (SCH_2). ^1H NMR (CDCl_3): δ 7.20 (m, 4H, aromatic), 4.31 (s, 4H, benzylic), 3.83 (t, 4H, CH_2O), 2.81 (t, 4H, SCH_2). Mp: 140–142 °C. Anal. Calcd for $\text{C}_{12}\text{H}_{16}\text{OS}_2$: C, 59.95; H, 6.72. Found: C, 59.81; H, 6.72.

General Preparation of $[\text{M}(\text{COD})(\text{L})][\text{BF}_4]$ Complexes. AgBF_4 (2 equiv) was weighed into a 50-mL Schlenk flask in a drybox, and then this flask was attached to a Schlenk line. $[\text{MCl}(\text{COD})_2]$ ($\text{M} = \text{Rh}, \text{Ir}$) (1 equiv) was added against the flow of $\text{N}_2(\text{g})$, followed by acetone. The resulting colored solution (orange or yellow) and white precipitate of $\text{AgCl}(\text{s})$ were stirred for 2 h, after which time the precipitate was allowed to settle. This solution was then filtered into a solution of thioether ligand (2 equiv) in acetone and stirred overnight. The volume of the resulting solution was reduced by ca. half and the desired product crystallized by diffusion of diethyl ether into the mother liquor.

Preparation of $[\text{Rh}(\text{COD})(\text{TT}[9]\text{OC})][\text{BF}_4]$ (1). Yield of orange microcrystals: 380 mg (76%). $^{13}\text{C}\{^1\text{H}\}$ NMR (acetone- d_6): δ 134.14, 131.09, 128.81 (aromatic), 79.66 (d, olefin, $J_{\text{Rh-C}} = 10.5$ Hz), 38.80 (benzylic), 36.57, 35.79 (CH_2S), 30.85 (COD CH_2). ^1H NMR (acetone- d_6): δ 7.44–7.34 (m, 4H, aromatic), 4.61 (m, 4H, benzylic, $J = 12.41$ Hz), 4.37 (m, 4H, SCH_2), 3.47 (s, 4H, olefin), 3.31–3.19 (m, 4H, CH_2S), 2.28 (br, 4H, COD CH_2), 1.81 (q, 4H, COD CH_2). Anal. Calcd for $\text{C}_{20}\text{H}_{28}\text{RhS}_3\text{BF}_4$: C, 43.33; H, 5.10. Found: C, 43.16; H, 5.03.

Preparation of $[\text{Ir}(\text{COD})(\text{TT}[9]\text{OC})][\text{BF}_4]$ (2). Yield of yellow microcrystals: 385 mg (77%). $^{13}\text{C}\{^1\text{H}\}$ NMR (acetone- d_6): δ 133.64, 131.13, 128.93 (aromatic), 64.48 (olefin), 40.52 (benzylic), 38.31, 38.03 (CH_2S), 32.34 (COD CH_2). ^1H NMR (acetone- d_6): δ 7.47–7.38 (m, 4H, aromatic), 4.64 (d, 2H, benzylic, $J = 11.47$ Hz), 4.24 (d, 2H, benzylic), 3.48 (m, 4H, SCH_2), 3.26 (m, 4H, CH_2S), 3.17 (br, 4H, olefin), 2.11 (br, 4H, COD CH_2), 1.81 (q, 4H, COD CH_2). Anal. Calcd for $\text{C}_{20}\text{H}_{28}\text{IrS}_3\text{BF}_4$: C, 37.32; H, 4.39. Found: C, 37.22; H, 4.33.

Preparation of $[\text{Rh}(\text{COD})(\text{ODT}[9]\text{OC})][\text{BF}_4]$ (3). Yield of orange microcrystals: 340 mg (68%). $^{13}\text{C}\{^1\text{H}\}$ NMR (acetone- d_6): δ 134.14, 130.91, 129.33 (aromatic), 85.19 (d, olefin, $J_{\text{Rh-C}} = 12.0$ Hz), 64.79 (OCH_2), 37.75 (benzylic), 35.85, (SCH_2), 31.15 (COD CH_2). ^1H NMR (acetone- d_6): δ 7.48 (s, 2H, aromatic), 4.31 (dd, 2H, benzylic, $J_{\text{Rh-H}} = 2.00$ Hz, $J = 11.85$ Hz), 4.27 (d, 2H, benzylic), 4.17 (m, 4H, OCH_2), 4.10 (s, 4H, olefin), 3.51–3.28 (m, 4H, CH_2S), 2.13, (br, 4H, COD CH_2), 1.90 (d, 4H, COD CH_2). Anal. Calcd for $\text{C}_{20}\text{H}_{28}\text{RhOS}_2\text{BF}_4$: C, 44.62; H, 5.25. Found: C, 44.95; H, 5.26.

Preparation of $[\text{Ir}(\text{COD})(\text{ODT}[9]\text{OC})][\text{BF}_4]$ (4). Yield of orange microcrystals: 325 mg (65%). $^{13}\text{C}\{^1\text{H}\}$ NMR (acetone- d_6): δ 134.49, 131.74, 130.02 (aromatic), 69.59 (olefin), 67.13 (OCH_2), 40.31 (benzylic), 36.52, (CH_2S), 32.36 (COD CH_2). ^1H NMR (acetone- d_6): δ 7.47 (m, 4H, aromatic), 4.84 (d, 2H, benzylic, $J = 11.88$ Hz), 4.49 (d, 2H, benzylic), 4.21 (m, 4H, OCH_2), 3.81–3.40 (m, 4H, CH_2S), 3.69 (br, 4H, olefin), 1.98 (br, 4H, COD CH_2),

1.65 (q, 4H, COD CH₂). Anal. Calcd for C₂₀H₂₈IrO₂S₂BF₄: C, 38.27; H, 4.51. Found: C, 38.62; H, 4.48.

Preparation of [Rh(CO)₂(TT[9]OB)][BF₄] (5) and [(TT[9]OC)Rh(μ-CO)₂Rh(TT[9]OC)][BF₄]₂ (6). 1 (20 mg, 0.0361 mmol) was dissolved in acetone (0.5 mL) under an atmosphere of CO(g) and stirred for 2 h, during which time the solution changed color from orange to orange-red. Stirring was stopped, and the solution was cooled to -20 °C for 48 h under CO(g) to precipitate an orange solid found to be a mixture of 5 and 6. Recrystallization of this solid under CO(g) yields a very small amount of 5: under N₂(g) 6 is obtained in 30% yield. 5: ¹H NMR (acetone-*d*₆) δ 7.66 (s, 4H, aromatic), 4.60 (d, 2H, benzylic, *J* = 12.40 Hz), 4.47 (d, 2H, benzylic), 3.63–3.20 (m, 8H, CH₂CH₂S); IR ν(CO) 2059, 1933 cm⁻¹. A satisfactory elemental analysis could not be obtained, as samples were consistently contaminated with 6. 6: ¹³C{¹H} NMR (acetone-*d*₆) δ 185.75, 184.86 (CO), 132.16, 131.74, 129.78 (aromatic), 37.69 (benzylic), 37.44, 37.11 (CH₂S); ¹H NMR (acetone-*d*₆) δ 7.51–7.41 (m, 4H, aromatic), 4.63 (dd, 2H, benzylic, *J* = 11.53, ³*J*_{Rh-H} = 2.13 Hz), 4.40 (d, 2H, benzylic), 3.79 (m, 2H, SCH₂), 3.61 (m, 4H, CH₂S), 3.33 (m, 2H, SCH₂); IR ν(CO) 1862, 1841 cm⁻¹. Anal. Calcd for C₂₇H₃₂S₆O₃Rh₂B₂F₈: C, 33.21; H, 3.31. Found: C, 33.17; H, 3.28.

Preparation of [Ir(CO)(COE)(TT[9]OC)][BF₄] (7). AgBF₄ (43 mg, 0.223 mmol) was weighed into a 50-mL Schlenk flask in a drybox, and then this flask was attached to a Schlenk line. [IrCl(COE)₂]₂ (100 mg, 0.112 mmol) was added as a solid, followed by acetone (25 mL). The resultant brown mixture was stirred for 1 h, and then TT[9]OC was added against the flow of N₂(g). The resulting yellow mixture was stirred for 2 h, and then the N₂(g) atmosphere was replaced by CO(g). Stirring was continued for 10 h, and then the mixture was filtered to yield a yellow solution. [Ir(CO)(COE)(TT[9]OC)]BF₄ was obtained by diffusion of diethyl ether into the mother liquor under an atmosphere of CO(g). Yield: 45 mg (61%). ¹³C{¹H} NMR (CD₃CN, 235 K): δ 184.34 (CO), 135.53, 131.62, 130.04 (aromatic), 65.95 (olefin), 41.19 (benzylic), 39.60, 34.66 (SCH₂CH₂S), 33.20, 31.80, 31.68 (COE). ¹H NMR (CD₃CN): δ 7.45 (s, 4H, aromatic), 4.72 (d, 2H, benzylic, *J* = 11.34 Hz), 4.44 (d, 2H, benzylic), 3.85 (m, 2H, olefin), 3.57 (m, 4H, CH₂S), 3.38 (m, 4H, SCH₂), 2.15 (m, 4H, COE), 1.60 (m, 4H, COE), 1.50 (s, 4H, COE). IR: ν(CO) 2073 cm⁻¹. Anal. Calcd for C₂₁H₃₀OIrS₃BF₄: C, 38.35; H, 4.61. Found: C, 38.27; H, 4.66.

Preparation of [Ir(CO)₂(TT[9]OC)][BF₄] (8). AgBF₄ (43 mg, 0.22 mmol) was weighed into a Schlenk flask in a drybox, and then this flask was transferred to a Schlenk line. [IrCl(COE)₂]₂ (100 mg, 0.112 mmol) was added as a solid against the flow of N₂(g). The atmosphere was changed to CO(g), and [IrCl(COE)₂]₂ began to darken. CH₃CN (10 mL) was added, resulting in an intensely blue-green precipitate and a pale yellow solution. This mixture was stirred for 30 min, and then TT[9]OC (57 mg, 0.22 mmol) was added as a solid against the flow of CO(g). The mixture gradually lightened in color, resulting in a yellow-orange solution and a gray AgCl precipitate. After it was stirred for 10 h under CO(g), the mixture was filtered to yield a yellow solution. The product was precipitated by diffusion of diethyl ether into the mother liquor. Yield of pale yellow microcrystals: 30 mg (46%). ¹³C{¹H} NMR (acetone-*d*₆): δ 166.68 (CO), 134.27, 131.99, 131.08 (aromatic), 41.11 (benzylic), 39.67, 36.60 (SCH₂). ¹H NMR (acetone-*d*₆): δ 7.75 (m, 4H, aromatic), 4.86 (d, 2H, benzylic, *J* = 11.76 ppm), 4.35 (d, 2H, benzylic), 3.90 (m, 2H, SCH₂), 3.67 (m, 4H, CH₂S), 3.48 (m, 2H, SCH₂). IR: ν(CO) 2095, 2045 cm⁻¹. Anal. Calcd for C₁₄H₁₆IrS₃O₂BF₄: C, 28.42; H, 2.73. Found: C, 28.33; H, 2.67.

Preparation of [Rh(CO)₃(ODT[9]OC)][BF₄] (9). 3 (20 mg, 0.0372 mmol) was dissolved in acetone (1 mL) under an atmosphere of CO(g) and the solution was stirred for 2 h, during which time it did not change color. The solution was cooled to -20 °C for 48 h, and a yellow-orange powder precipitated. After the mother liquor was removed by syringe, the precipitate was washed with diethyl ether to remove COD and then dried *in vacuo*. Yield: 8 mg, 42%. ¹³C{¹H} NMR (acetone-*d*₆, 210 K): δ 179.97, 179.03 (CO), 132.51, 130.79, 130.12 (aromatic), 64.22

(OCH₂), 39.27 (benzylic), 38.29 (SCH₂). ¹H NMR (acetone-*d*₆, 210 K): δ 7.48 (s, 4H, aromatic), 4.58 (d, 2H, benzylic, *J* = 11.73 Hz), 4.26 (d, 2H, benzylic), 4.12 (m, 4H, OCH₂), 3.82 (m, 4H, SCH₂). IR: ν(CO) 2103, 2044, 2015 cm⁻¹. Anal. Calcd for C₁₅H₁₆O₄S₂RhBF₄: C, 35.04; H, 3.14. Found: C, 34.93; H, 3.11.

Preparation of [Ir(CO)₃(ODT[9]OC)][BF₄] (10). 4 (20 mg, 0.0319 mmol) was dissolved in acetone (0.5 mL) and stirred under an atmosphere of CO(g) for 30 min. The solution changed color from orange to red to dark orange, and a yellow powder precipitated from solution after about 10 min. The product was filtered, washed with diethyl ether to remove free COD, and dried *in vacuo*. Yield: 12 mg, 62%. ¹³C{¹H} NMR (CD₃CN): δ 169.65, 168.37, 157.68 (CO), 133.42, 132.45, 130.04 (aromatic), 80.52, 77.17 (CH₂O), 44.29, 37.38 (benzylic), 37.18, 34.38 (CH₂S). ¹H NMR (CD₃CN): δ 7.62–7.46 (m, 4H, aromatic), 5.06 (d, 1H, benzylic, *J* = 11.96 Hz), 4.88 (d, 1H, benzylic, *J* = 11.75 Hz), 4.74 (ddd, 1H, OCH₂), 4.44 (m, 1H, OCH₂), 4.27 (m, 2H, benzylic, *J* = 11.70 Hz), 3.98 (dt, 1H, OCH₂), 3.49 (m, 1H, OCH₂), 3.39 (q, 1H, SCH₂), 3.34 (q, 1H, SCH₂), 3.23 (ddd, 1H, SCH₂), 3.02 (dq, 1H, SCH₂). IR: ν(CO) 2024 (br) cm⁻¹. Anal. Calcd for C₁₅H₁₆O₄S₂IrBF₄: C, 29.85; H, 2.68. Found: C, 29.76; H, 2.58.

Preparation of [Rh(COD)(NO)(TT[9]OC)][BF₄]₂ (11). 1 (20 mg, 0.0372 mmol) was weighed into an NMR tube and NOBF₄ (5 mg, 0.0423 mmol) added as a solid. The tube was capped and placed under an atmosphere of N₂(g). Acetone-*d*₆ was added and the ¹H NMR spectrum of the resultant brown solution recorded immediately. ¹H NMR (acetone-*d*₆): δ 7.67 (m, 4H, aromatic), 6.37 (br, 2H, olefinic), 5.88 (br, 2H, olefinic), 5.41 (d, 2H, benzylic, *J* = 14.69 Hz), 4.54 (dd, benzylic, *J*_{Rh-H} = 1.6 Hz), 4.83 (m, 4H, SCH₂), 3.96 (m, 4H, SCH₂), 3.62 (m, 4H, COD CH₂), 3.08 (m, 2H, COD CH₂), 2.78 (m, 2H, COD CH₂). This compound was completely decomposed within 15 min of mixing with apparent loss of cyclooctadiene detected by ¹H NMR spectroscopy. No pure solid product could be isolated before this decomposition occurred.

Preparation of [Ir(COD)(NO)(TT[9]OC)][BF₄]₂ (12). 2 (20 mg, 0.032 mmol) was weighed into an NMR tube, and NOBF₄ (4 mg, 0.04 mmol) was added as a solid. The tube was capped and placed under an N₂(g) atmosphere. Acetone-*d*₆ was added, and the ¹H NMR spectrum of the resultant bright yellow solution was recorded immediately. NMR spectra (acetone-*d*₆) clearly showed two products in a 1:1 ratio: **12a**: ¹H NMR (acetone-*d*₆) δ 7.81 (m, 2H, aromatic), 7.61 (m, 2H, aromatic), 5.23 (m, 4H, olefin), 5.11 (d, 2H, benzylic, *J* = 12.42 Hz), 4.87 (d, 2H, benzylic), 4.06 (m, 4H, SCH₂), 3.74 (m, 2H, CH₂S), 3.60 (m, 2H, CH₂S), 2.55 (m, 4H, COD CH₂), 2.33 (m, 4H, COD CH₂); ¹³C{¹H} NMR (acetone-*d*₆) δ 140.40, 137.67, 136.01 (aromatic), 114.43, 95.02 (COD olefin), 44.29 (benzylic), 43.44 (SCH₂), 39.75, 38.88 (COD aliphatic). **12b**: ¹H NMR (acetone-*d*₆) δ 7.42 (s, br, 4H, aromatic), 5.68 (m, 2H, olefin), 5.55 (m, 2H, olefin), 4.71 (d, 2H, benzylic, *J* = 14.67 Hz), 4.19 (d, 2H, benzylic), 4.06 (m, 4H, SCH₂), 3.41 (m, 2H, CH₂S), 3.21 (m, 2H, CH₂S), 2.10 (m, 4H, COD CH₂), 1.86 (m, 4H, COD CH₂); ¹³C{¹H} NMR (acetone-*d*₆) δ 137.06, 135.87, 136.01 (aromatic), 115.94, 94.18 (COD olefin), 45.96 (benzylic), 43.56 (SCH₂), 41.49 (CH₂S), 40.95 (COD aliphatic); IR (CH₃CN) ν(NO) 1678, 1639 cm⁻¹. This compound completely decomposed within 15 min of mixing with apparent loss of cyclooctadiene, as detected by ¹H NMR spectroscopy. No pure solid product could be isolated before this decomposition occurred.

Preparation of [Rh(COD)(NO)(ODT[9]OC)][BF₄]₂ (13). 3 (20 mg, 0.0372 mmol) was weighed into an NMR tube, and NOBF₄ (4 mg, 0.04 mmol) was added as a solid. The tube was capped and placed under an N₂(g) atmosphere. Acetone-*d*₆ was added, and the NMR spectrum of the resultant dark green solution was recorded immediately. NMR spectra (acetone-*d*₆) clearly showed two products were present in a 1:3 ratio. **13a**: ¹H NMR (acetone-*d*₆) δ 7.81 (m, 2H, aromatic), 7.63 (m, 2H, aromatic), 6.08 (m, 2H, olefin), 5.94 (m, 2H, olefin), 4.94 (dd, 2H, benzylic, *J* = 12.47 Hz, *J*_{Rh-H} = 2.74 Hz), 4.81 (d, 2H, benzylic), 4.33 (m, 4H, OCH₂), 3.54–3.21 (m, 4H, CH₂S), 2.53 (br, 4H, COD CH₂), 2.25 (br, 4H, COD CH₂); ¹³C{¹H} NMR (acetone-*d*₆) δ 140.94, 136.99, 136.61 (aromatic), 126.16, 120.50 (olefin), 74.16 (CH₂O),

Table 1. Summary of Crystal Data, Intensity Collection, and Structure Refinement

	1	2	3	4	7	14
formula	C ₂₀ H ₂₈ BF ₄ RhS ₃	C ₂₀ H ₂₈ BF ₄ IrS ₃	C ₂₀ H ₂₈ BF ₄ ORhS ₂	C ₂₀ H ₂₈ BF ₄ IrOS ₂	C ₄₅ H ₅₀ BIrOS ₃	C ₂₀ H ₂₈ B ₂ F ₈ IrNO ₂ S ₂
fw	554.30	643.61	538.24	627.55	906.16	744.37
a, Å	23.951(4)	11.085(6)	9.173(2)	9.677(3)	23.338(5)	18.821(6)
b, Å	8.845(2)	12.649(2)	24.173(6)	13.142(6)	24.646(9)	9.611(5)
c, Å	10.463(8)	7.965(2)	9.907(3)	8.996(2)	13.805(5)	14.225(8)
α, deg		103.10(1)		107.48(3)		
β, deg		93.93(3)	94.14(3)	92.87(3)		
γ, deg		89.45(2)		97.46(3)		
space group	<i>Pca</i> 2 ₁ (No. 29)	<i>P</i> $\bar{1}$ (No. 2)	<i>P</i> 2 ₁ / <i>c</i> (No. 14)	<i>P</i> $\bar{1}$ (No. 2)	<i>Pbca</i> (No. 61)	<i>Pnma</i> (No. 62)
V, Å ³	2217(1)	1085.2(5)	2190(2)	1077.2(7)	7940(4)	2573(2)
ρ, g cm ⁻³	1.661	1.970	1.632	1.930	1.516	1.921
Z	4	2	4	2	8	4
μ, cm ⁻¹	10.669	64.459	9.914	64.510	35.348	53.97
transmissn factor	0.9533	0.8393	0.9879	0.8173	0.8830	0.9954
diffractometer	AFC6S	AFC6S	AFC6S	AFC6S	AFC6S	AFC6S
λ, Å	0.710 69	0.710 69	0.710 69	0.710 69	0.710 69	0.710 69
T, °C	24	24	24	24	24	24
no. of data collected	2277	3823	4233	4047	6726	2603
no. of data with F _o ² > 3σ(F _o ²)	1192	2935	2312	3802	1493	1180
no. of variables	161	263	263	262	176	152
goodness of fit	1.72	1.49	1.85	2.95	1.73	1.79
R(F _o), %	5.26	4.06	5.84	7.38	7.68	5.11
R _w (F _o), %	5.70	4.41	6.87	6.59	7.98	4.83

$$^a R = \sum |F_o| - |F_c| / \sum |F_o|, R_w = (\sum w(|F_o| - |F_c|)^2 / \sum w F_o^2)^{1/2}, \text{ and } w = 1/\sigma^2(F).$$

41.87 (benzylic), 41.07 (CH₂S), 38.73 (COD CH₂). **13b**: ¹H NMR (acetone-*d*₆) δ 7.43 (s, 4H, aromatic), 6.49 (br, 2H, olefin), 6.23 (br 2H, olefin), 4.70 (dd, 2H, benzylic, *J* = 14.63 Hz, *J*_{Rh-H} = 2.28 Hz), 4.56 (t, 4H, OCH₂), 4.33 (d, 2H, benzylic), 4.12 (t, 4H, CH₂S), 2.81 (m, 4H, COD CH₂), 2.61 (m, 4H, COD CH₂); ¹³C{¹H} NMR (acetone-*d*₆) δ 137.55, 136.11, 135.28 (aromatic), 128.29, 120.93 (olefin), 71.29 (OCH₂), 44.51 (benzylic), 42.95 (CH₂S), 40.67 (COD CH₂); IR (CH₃CN) ν(NO) 1712, 1671 cm⁻¹. This compound was completely decomposed within 15 min of mixing with apparent loss of cyclooctadiene, as detected by ¹H NMR spectroscopy. No pure solid product could be isolated before this decomposition occurred.

Preparation of [Ir(COD)(NO)(ODT[9]OC)][BF₄]₂ (14). **4** (100 mg, 0.159 mmol) and NOBF₄ (19 mg, 0.160 mmol) were weighed out and placed in a flask under N₂(g). Acetone (5 mL) was added and the resultant dark green solution stirred for 5 min. Diethyl ether was added until a small amount of precipitate formed and the mixture cooled to -20 °C for 10 h to give **14** as well-formed dark green crystals suitable for single-crystal X-ray analysis. Yield: 50 mg, 43%. After this initial crystallization, further product could not be isolated due to decomposition. Dissolution of the green crystals from the sample used for diffraction study showed two products in solution in a 1:2 ratio. **14a**: ¹H NMR (acetone-*d*₆) δ 7.85 (m, 2H, aromatic), 7.66 (m, 2H, aromatic), 5.98 (br m, 2H, olefin), 5.92 (br m, 2H, olefin), 5.11 (d, 2H, benzylic, *J* = 14.39 Hz), 4.39 (d, 2H, benzylic), 3.77 (m, 4H, OCH₂), 3.73 (m, 2H, CH₂S), 3.30 (m, 2H, CH₂S), 2.76 (m, 4H, COD CH₂), 2.25 (m, 4H, COD CH₂); ¹³C{¹H} NMR (acetone-*d*₆) δ 136.19, 131.43, 133.11 (aromatic), 109.82, 104.40 (olefin), 68.28 (CH₂O), 37.61 (benzylic), 37.44 (CH₂S), 29.35 (COD CH₂). **14b**: ¹H NMR (acetone-*d*₆) δ 7.43 (s, 4H, aromatic), 6.36 (m, 2H, olefin), 5.98 (m, 2H, olefin), 5.25 (d, 2H, benzylic, *J* = 12.44 Hz), 5.10 (d, 2H, benzylic), 4.75–4.63 (m, 4H, OCH₂), 4.32 (m, 4H, CH₂S), 2.59 (COD CH₂), 2.45 (COD CH₂); ¹³C{¹H} NMR (acetone-*d*₆) δ 133.09, 131.61, 130.63 (aromatic), 110.92, 103.33 (olefin), 68.28 (CH₂O), 40.85 (benzylic), 39.66 (CH₂S), 29.49 (COD CH₂); IR (KBr) ν(NO) 1708 cm⁻¹; IR (CH₃CN) ν(NO) 1695, 1655 cm⁻¹. Anal. Calcd for C₂₀H₂₈IrO₂NS₂B₂F₈: C, 32.27; H, 3.80. Found: C, 32.12; H, 3.89.

General X-ray Diffraction Data Collection, Solution, and Refinement Conditions. Orange crystals of **1** and yellow crystals of **2** were grown by diffusion of diethyl ether into an acetonitrile solution of the complex, orange crystals of **3** and **4** were grown by diffusion of diethyl ether into an acetone solution of the complex, orange crystals of **7** were grown by diffusion of diethyl ether into an acetone solution of the complex saturated with

Table 2. Selected Positional Parameters and B(eq) Values for [Rh(1,5-COD)(TT[9]OC)][BF₄]

atom	x	y	z	B(eq), Å ²
Rh	0.09959(4)	0.2439(1)	0	3.37(4)
S(1)	0.1974(2)	0.1746(5)	-0.0024(8)	4.0(2)
S(2)	0.0816(2)	-0.0121(6)	0.0216(6)	5.1(3)
S(3)	0.0797(2)	0.2588(7)	0.2337(5)	4.7(2)
C(7)	0.2346(9)	0.211(2)	0.151(2)	7.2(6)
C(8)	0.1950(9)	-0.030(2)	-0.004(3)	8.4(6)
C(9)	0.144(1)	-0.105(3)	-0.024(3)	9.2(7)
C(10)	0.073(1)	-0.043(3)	0.196(3)	9.5(8)
C(11)	0.0497(9)	0.076(3)	0.265(2)	6.7(6)
C(12)	0.1434(9)	0.261(2)	0.337(2)	6.7(5)
C(13)	0.1289(8)	0.456(2)	-0.094(2)	5.0(4)
C(14)	0.0961(7)	0.489(2)	0.014(3)	4.8(4)
C(15)	0.0339(9)	0.534(2)	0.005(3)	7.5(5)
C(16)	-0.0046(9)	0.431(2)	-0.057(2)	5.4(5)
C(17)	0.0198(7)	0.275(2)	-0.083(2)	4.2(4)
C(18)	0.0556(8)	0.227(2)	-0.173(2)	4.6(4)
C(19)	0.083(1)	0.332(3)	-0.271(3)	7.6(7)
C(20)	0.106(1)	0.459(3)	-0.235(3)	7.4(6)

CO(g), and emerald green crystals of **14** were grown by cooling a 1:1 diethyl ether/acetone solution of the complex to -20 °C. Diffraction experiments were performed on a four-circle Rigaku AFC6S diffractometer with graphite-monochromatized Mo Kα radiation. The unit cell constants and orientation matrices for data collection were obtained from 25 centered reflections (15° < 2θ < 35°). Machine parameters, crystal data, and data collection parameters are summarized in Tables 1 and S-I (supplementary material). The intensities of 3 standard reflections were recorded every 150 reflections and showed no statistically significant changes over the duration of the data collections. The intensity data were collected using the ω-2θ scan technique, in four shells (2θ < 30, 40, 45, and 50°). Absorption coefficients were calculated and corrections applied to the data. The data were processed using the TEXSAN software²⁰ package running on a VAX 3520 or SGI computer. For each solution, the position of the metal atom was determined by conventional Patterson methods and the remaining non-hydrogen atoms located from a series of difference Fourier map calculations. Refinements were carried out by using full-matrix least-squares techniques on *F* by minimizing the function $\sum w(F_o - F_c)^2$, where $w = 1/\sigma^2(F_o)$ and F_o and F_c are the observed and calculated structure factors. Atomic scattering factors²¹ and anomalous dispersion terms^{22,23} were taken

(20) TEXSAN-TEXRAY Structure Analysis Package, Molecular Structure Corp., 1985.

Table 3. Selected Bonding Parameters for [Rh(1,5-COD)(TT[9]OC)][BF₄]

Distances (Å)			
Rh-S(1)	2.422(4)	Rh-S(2)	2.316(5)
Rh-S(3)	2.494(5)	Rh-C(13)	2.23(2)
Rh-C(14)	2.18(2)	Rh-C(17)	2.12(2)
Rh-C(18)	2.10(2)	S(1)-C(7)	1.86(2)
S(1)-C(8)	1.81(2)	S(2)-C(9)	1.76(2)
S(2)-C(10)	1.86(3)	S(3)-C(11)	1.80(2)
S(3)-C(12)	1.87(2)	C(1)-C(12)	1.47(2)
C(6)-C(7)	1.45(2)	C(8)-C(9)	1.41(3)
C(10)-C(11)	1.39(3)		
Angles (deg)			
S(1)-Rh-S(2)	86.2(2)	S(1)-Rh-S(3)	102.0(2)
S(2)-Rh-S(3)	85.5(2)	S(1)-Rh-C(13)	84.5(5)
S(1)-Rh-C(14)	106.9(4)	S(1)-Rh-C(17)	154.4(5)
S(1)-Rh-C(18)	117.3(6)	S(2)-Rh-C(13)	157.3(5)
S(2)-Rh-C(14)	164.0(6)	S(2)-Rh-C(17)	89.9(5)
S(2)-Rh-C(18)	85.5(5)	S(3)-Rh-C(13)	116.7(5)
S(3)-Rh-C(14)	82.8(7)	S(3)-Rh-C(17)	102.9(5)
S(3)-Rh-C(18)	138.9(6)	C(13)-Rh-C(14)	37.2(8)
C(13)-Rh-C(17)	89.6(7)	C(13)-Rh-C(18)	80.5(7)
C(14)-Rh-C(17)	82.1(7)	C(14)-Rh-C(18)	96.1(8)
C(17)-Rh-C(18)	37.1(6)	C(7)-S(1)-C(8)	101(1)
C(9)-S(2)-C(10)	107(1)	C(11)-S(3)-C(12)	104(1)

Table 4. Selected Positional Parameters and *B*(eq) Values for [Ir(1,5-COD)(TT[9]OC)][BF₄]

atom	<i>x</i>	<i>y</i>	<i>z</i>	<i>B</i> (eq), Å ²
Ir	0.21548(4)	0.36124(3)	0.20559(5)	3.16(2)
S(1)	0.3260(3)	0.2750(2)	0.4143(3)	4.1(1)
S(2)	0.0405(3)	0.3059(2)	0.3050(4)	5.1(1)
S(3)	0.1831(2)	0.2096(2)	-0.0309(3)	3.4(1)
C(7)	0.416(1)	0.1527(8)	0.336(1)	4.7(5)
C(8)	0.206(1)	0.214(1)	0.507(1)	6.1(6)
C(9)	0.089(1)	0.278(1)	0.513(2)	7.2(7)
C(10)	0.008(1)	0.172(1)	0.174(2)	5.7(6)
C(11)	0.032(1)	0.1634(8)	-0.008(2)	5.1(5)
C(12)	0.272(1)	0.0915(7)	-0.004(1)	4.3(4)
C(13)	0.320(2)	0.423(1)	0.027(2)	7.4(8)
C(14)	0.388(1)	0.439(1)	0.178(2)	7.7(8)
C(15)	0.403(2)	0.550(1)	0.298(3)	9(1)
C(16)	0.311(2)	0.577(1)	0.429(2)	11(1)
C(17)	0.193(1)	0.5170(8)	0.367(2)	6.1(6)
C(18)	0.131(1)	0.5120(8)	0.205(2)	5.4(5)
C(19)	0.172(1)	0.574(1)	0.077(2)	7.5(7)
C(20)	0.253(2)	0.508(1)	-0.039(2)	8.4(9)

from the usual sources. In the final cycles of refinement, the iridium, rhodium, sulfur, fluorine, oxygen, nitrogen, and boron atoms were assigned anisotropic thermal parameters and carbon atoms were assigned isotropic thermal parameters, except for 14, for which all atoms were assigned anisotropic thermal parameters. Fixed H atom contributions were included with C-H distances of 0.95 Å and thermal parameters 1.2 times the isotropic thermal parameter of the bonded C atoms. No H atoms were refined, but all values were updated as refinement continued. Selected atomic positional parameters are summarized in Tables 2, 4, 6, 8, 10, and 12 and selected bonding parameters are summarized in Tables 3, 5, 7, 9, 11, and 13. Full listings of atomic positional parameters (Tables S-II, S-VI, S-X, S-XIV, S-XVIII, and S-XXII), nonessential bonding parameters (Tables S-III, S-VII, S-XI, S-XV, S-XIX, and S-XXIII), thermal parameters (Tables S-IV, S-VIII, S-XII, S-XVI, S-XX, and S-XXIV), and hydrogen atom parameters (Tables S-V, S-IX, S-XIII, S-XVII, S-XXI, and S-XXV) are deposited as supplementary material.

(21) Cromer, D. T.; Waber, J. T. *International Tables for X-ray Crystallography*; Kynoch Press: Birmingham, U.K., 1974; Vol. IV, Table 2.2A.

(22) Ibers, J. A.; Hamilton, W. C. *Acta Crystallogr.* 1964, 17, 781.

(23) Cromer, D. T. *International Tables for X-ray Crystallography*; Kynoch Press: Birmingham, U. K., 1974; Vol. IV, Table 2.3.1.

Table 5. Selected Bond Distances and Angles for [Ir(1,5-COD)(TT[9]OC)][BF₄]

Distances (Å)			
Ir-S(1)	2.444(3)	Ir-S(2)	2.317(3)
Ir-S(3)	2.375(2)	Ir-C(13)	2.17(1)
Ir-C(14)	2.20(1)	Ir-C(17)	2.12(1)
Ir-C(18)	2.12(1)	S(1)-C(7)	1.84(1)
S(1)-C(8)	1.82(1)	S(2)-C(9)	1.81(1)
S(2)-C(10)	1.80(1)	S(3)-C(11)	1.81(1)
S(3)-C(12)	1.83(1)	C(1)-C(12)	1.51(1)
C(6)-C(7)	1.48(1)	C(8)-C(9)	1.52(2)
C(10)-C(11)	1.48(2)		
Angles (deg)			
S(1)-Ir-S(2)	86.7(1)	S(1)-Ir-S(3)	100.33(8)
S(2)-Ir-S(3)	85.8(1)	S(1)-Ir-C(17)	98.7(3)
S(1)-Ir-C(18)	137.5(3)	S(1)-Ir-C(13)	117.6(5)
S(1)-Ir-C(14)	87.1(4)	S(2)-Ir-C(17)	88.6(4)
S(2)-Ir-C(18)	88.1(4)	S(2)-Ir-C(13)	154.9(5)
S(2)-Ir-C(14)	165.5(5)	S(3)-Ir-C(17)	159.8(4)
S(3)-Ir-C(14)	121.3(3)	S(3)-Ir-C(13)	83.6(4)
S(3)-Ir-C(18)	108.2(5)	C(17)-Ir-C(18)	39.0(4)
C(17)-Ir-C(13)	93.6(5)	C(17)-Ir-C(14)	79.4(6)
C(18)-Ir-C(13)	78.3(6)	C(18)-Ir-C(14)	87.7(4)
C(13)-Ir-C(14)	36.0(5)	C(7)-S(1)-C(8)	113.1(9)
C(9)-S(2)-C(10)	102.3(6)	C(11)-S(3)-C(12)	100.7(5)

Table 6. Selected Positional Parameters and *B*(eq) Values for [Rh(1,5-COD)(DTO[9]OC)][BF₄]

atom	<i>x</i>	<i>y</i>	<i>z</i>	<i>B</i> (eq), Å ²
Rh	0.12433(9)	0.09525(3)	0.26957(8)	2.73(3)
S(1)	-0.1281(3)	0.0728(1)	0.2593(3)	3.9(1)
S(2)	0.1168(3)	0.1854(1)	0.1606(3)	3.3(1)
O(1)	0.0455(9)	0.0790(3)	0.0029(8)	4.5(4)
C(7)	-0.242(1)	0.1343(5)	0.264(1)	4.4(6)
C(8)	-0.174(1)	0.0463(5)	0.091(2)	5.8(7)
C(9)	-0.109(1)	0.0773(6)	-0.019(1)	5.9(8)
C(10)	0.113(1)	0.1213(6)	-0.071(1)	5.5(7)
C(11)	0.081(1)	0.1797(6)	-0.022(1)	5.1(7)
C(12)	-0.038(1)	0.2278(5)	0.207(1)	4.5(6)
C(13)	0.354(1)	0.0915(6)	0.243(1)	4.7(6)
C(14)	0.340(1)	0.1222(4)	0.353(1)	3.4(5)
C(15)	0.375(2)	0.1032(6)	0.498(1)	6.2(8)
C(16)	0.244(2)	0.0810(7)	0.559(1)	6.8(9)
C(17)	0.135(1)	0.0529(5)	0.458(1)	4.6(6)
C(18)	0.166(1)	0.0165(5)	0.358(1)	4.3(6)
C(19)	0.318(1)	-0.0049(5)	0.338(1)	5.6(7)
C(20)	0.398(1)	0.0313(6)	0.245(1)	5.8(7)

Table 7. Selected Bonding Parameters for [Rh(1,5-COD)(ODT[9]OC)][BF₄]

Distances (Å)			
Rh-S(1)	2.373(3)	Rh-S(2)	2.431(3)
Rh-C(13)	2.15(1)	Rh-C(14)	2.19(1)
Rh-C(17)	2.12(1)	Rh-C(18)	2.12(1)
S(1)-C(7)	1.82(1)	S(1)-C(8)	1.80(1)
S(2)-C(11)	1.82(1)	S(2)-C(12)	1.84(1)
O(1)-C(9)	1.42(1)	O(1)-C(10)	1.42(2)
C(1)-C(12)	1.52(2)	C(6)-C(7)	1.50(1)
C(8)-C(9)	1.48(2)	C(10)-C(11)	1.53(2)
Angles (deg)			
S(1)-Rh-S(2)	100.9(1)	S(1)-Rh-C(13)	161.7(4)
S(1)-Rh-C(14)	159.5(3)	S(1)-Rh-C(17)	84.8(3)
S(1)-Rh-C(18)	87.7(3)	S(2)-Rh-C(13)	88.8(3)
S(2)-Rh-C(14)	84.1(3)	S(2)-Rh-C(17)	145.1(4)
S(2)-Rh-C(18)	170.9(3)	C(13)-Rh-C(14)	36.0(4)
C(13)-Rh-C(17)	96.1(5)	C(13)-Rh-C(18)	82.1(5)
C(14)-Rh-C(17)	80.1(4)	C(14)-Rh-C(18)	88.8(4)
C(17)-Rh-C(18)	37.8(4)	C(7)-S(1)-C(8)	102.7(6)
C(11)-S(2)-C(12)	101.9(6)	C(9)-O(1)-C(10)	114(1)

Results and Discussion

Synthesis of [ODT[9]OC]. ODT[9]OC was prepared in ca. 80% yield by employing the Cs⁺-mediated synthesis

Table 8. Selected Positional Parameters and $B(\text{eq})$ Values for $[\text{Ir}(\text{1,5-COD})(\text{ODT}[9]\text{OC})][\text{BF}_4]$

atom	x	y	z	$B(\text{eq}), \text{\AA}^2$
Ir	0.29059(9)	0.18521(7)	0.22036(9)	2.37(2)
S(1)	0.2161(5)	0.3592(4)	0.3161(6)	3.5(2)
S(2)	0.2943(6)	0.1666(5)	-0.0472(6)	3.7(2)
O(1)	0.027(2)	0.156(1)	0.128(2)	4.3(6)
C(7)	0.291(2)	0.454(2)	0.217(2)	4.0(9)
C(8)	0.027(2)	0.346(2)	0.267(3)	5(1)
C(9)	-0.042(3)	0.229(2)	0.233(3)	6(1)
C(10)	0.015(3)	0.165(2)	-0.023(3)	7(1)
C(11)	0.116(3)	0.103(2)	-0.125(2)	7(1)
C(12)	0.320(2)	0.297(2)	-0.085(2)	4.1(9)
C(13)	0.486(2)	0.136(2)	0.203(3)	5(1)
C(14)	0.383(3)	0.051(2)	0.172(3)	5(1)
C(15)	0.359(3)	-0.028(2)	0.275(3)	6(1)
C(16)	0.250(2)	0.018(2)	0.390(3)	4(1)
C(17)	0.245(2)	0.135(2)	0.420(2)	3.9(9)
C(18)	0.358(2)	0.222(2)	0.470(2)	5(1)
C(19)	0.510(2)	0.196(2)	0.485(3)	7(1)
C(20)	0.587(3)	0.181(3)	0.355(3)	10(1)

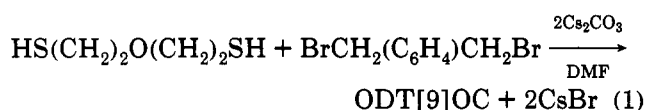
Table 9. Selected Bonding Parameters for $[\text{Ir}(\text{1,5-COD})(\text{ODT}[9]\text{OC})][\text{BF}_4]$

Distances (\AA)			
Ir-S(1)	2.407(6)	Ir-S(2)	2.348(5)
Ir-C(13)	2.08(2)	Ir-C(14)	2.02(3)
Ir-C(17)	2.14(2)	Ir-C(18)	2.20(2)
S(1)-C(7)	1.84(2)	S(1)-C(8)	1.84(2)
S(2)-C(11)	1.82(2)	S(2)-C(12)	1.83(2)
O(1)-C(9)	1.40(3)	O(1)-C(10)	1.40(2)
C(1)-C(12)	1.49(3)	C(6)-C(7)	1.47(3)
C(8)-C(9)	1.54(3)	C(10)-C(11)	1.53(4)
Angles (deg)			
S(1)-Ir-S(2)	100.8(2)	S(1)-Ir-C(13)	133.1(7)
S(1)-Ir-C(14)	169.3(7)	S(1)-Ir-C(17)	96.2(6)
S(1)-Ir-C(18)	81.4(7)	S(2)-Ir-C(13)	85.0(6)
S(2)-Ir-C(14)	85.7(6)	S(2)-Ir-C(17)	156.0(6)
S(2)-Ir-C(18)	161.7(6)	C(13)-Ir-C(14)	38.4(9)
C(13)-Ir-C(17)	95.5(8)	C(13)-Ir-C(18)	80.5(9)
C(14)-Ir-C(17)	80.1(9)	C(14)-Ir-C(18)	89.8(9)
C(17)-Ir-C(18)	38.2(8)	C(7)-S(1)-C(8)	103(1)
C(11)-S(2)-C(12)	107(1)	C(9)-O(1)-C(10)	113(2)

Table 10. Selected Positional Parameters and $B(\text{eq})$ Values for $[\text{Ir}(\text{COE})(\text{CO})(\text{TT}[9]\text{OC})][\text{BPh}_4]$

atom	x	y	z	$B(\text{eq}), \text{\AA}^2$
Ir	0.08778(8)	0.16344(7)	0.2011(1)	3.37(7)
S(1)	0.1882(5)	0.1682(5)	0.1688(8)	4.2(6)
S(2)	0.0866(7)	0.0821(5)	0.112(1)	6.2(8)
S(3)	0.0762(5)	0.1069(4)	0.3427(8)	4.1(7)
O(1)	0.097(1)	0.268(1)	0.305(2)	6.5(8)
C(7)	0.228(2)	0.129(2)	0.260(3)	5(1)
C(8)	0.193(2)	0.126(2)	0.064(4)	7(1)
C(9)	0.159(2)	0.071(2)	0.070(4)	8(2)
C(10)	0.078(2)	0.029(2)	0.215(4)	7(1)
C(11)	0.047(2)	0.046(2)	0.299(4)	6(1)
C(12)	0.143(2)	0.081(2)	0.396(3)	5(1)
C(13)	0.091(2)	0.222(2)	0.265(3)	4(1)
C(14)	0.042(2)	0.192(2)	0.074(3)	5(1)
C(15)	-0.000(2)	0.172(2)	0.151(3)	3(1)
C(16)	-0.038(2)	0.204(2)	0.219(4)	6(1)
C(17)	-0.099(2)	0.215(2)	0.171(3)	6(1)
C(18)	-0.094(2)	0.253(2)	0.088(4)	7(1)
C(19)	-0.070(2)	0.236(2)	-0.001(4)	9(2)
C(20)	-0.010(2)	0.267(2)	-0.019(4)	8(2)
C(21)	0.038(2)	0.254(2)	0.061(3)	5(1)

of Buter and Kellogg²⁴ as outlined in eq 1. This is a



convenient one-step synthesis from commercially available

Table 11. Selected Bonding Parameters for $[\text{Ir}(\text{COE})(\text{CO})(\text{TT}[9]\text{OC})][\text{BF}_4]$

Distances (\AA)			
Ir-S(1)	2.39(1)	Ir-S(2)	2.35(1)
Ir-S(3)	2.41(1)	Ir-C(13)	1.70(4)
Ir-C(14)	2.17(5)	Ir-C(15)	2.18(4)
S(1)-C(7)	1.85(4)	S(1)-C(8)	1.78(5)
S(2)-C(9)	1.82(6)	S(2)-C(10)	1.94(5)
S(3)-C(11)	1.76(5)	S(3)-C(12)	1.84(5)
O(1)-C(13)	1.27(5)	C(1)-C(12)	1.45(6)
C(6)-C(7)	1.49(6)	C(8)-C(9)	1.59(7)
C(10)-C(11)	1.44(7)		
Angles (deg)			
S(1)-Ir-S(2)	87.5(5)	S(1)-Ir-S(3)	106.8(4)
S(2)-Ir-S(3)	85.9(4)	S(1)-Ir-C(13)	91(2)
S(1)-Ir-C(14)	108(1)	S(1)-Ir-C(15)	149(1)
S(2)-Ir-C(13)	178(2)	S(2)-Ir-C(14)	81(1)
S(2)-Ir-C(15)	85(1)	S(3)-Ir-C(13)	94(1)
S(3)-Ir-C(14)	142(1)	S(3)-Ir-C(15)	102(1)
C(13)-Ir-C(14)	100(2)	C(13)-Ir-C(15)	97(2)
C(14)-Ir-C(15)	41(2)	C(7)-S(1)-C(8)	102(2)
C(9)-S(2)-C(10)	103(2)	C(11)-S(3)-C(12)	100(2)

Table 12. Selected Positional Parameters and $B(\text{eq})$ Values for $[\text{Ir}(\text{1,5-COD})(\text{NO})(\text{ODT}[9]\text{OC})][\text{BF}_4]$

atom	x	y	z	$B(\text{eq}), \text{\AA}^2$
Ir	0.36216(7)	1/4	0.15916(8)	2.34(4)
S(1)	0.3006(3)	0.0580(5)	0.2262(3)	3.6(2)
O(1)	0.281(2)	0.311(3)	-0.007(2)	6(2)
O(2)	0.404(1)	1/4	0.330(2)	5(1)
N(1)	0.292(1)	1/4	0.054(2)	5(2)
C(4)	0.210(1)	0.094(2)	0.258(2)	5.3(5)
C(5)	0.340(1)	0.028(2)	0.338(2)	5.8(5)
C(6)	0.389(2)	0.125(3)	0.370(2)	10(1)
C(7)	0.519(1)	0.172(2)	0.155(2)	6.4(6)
C(8)	0.450(1)	0.102(2)	0.140(1)	3.7(4)
C(9)	0.413(1)	0.100(2)	0.058(1)	4.0(4)
C(10)	0.444(1)	0.170(3)	-0.028(2)	7.1(7)

Table 13. Selected Bonding Parameters for $[\text{Ir}(\text{1,5-COD})(\text{NO})(\text{ODT}[9]\text{OC})][\text{BF}_4]$

Distances (\AA)			
Ir-S(1)	2.378(5)	Ir-N(1)	1.99(3)
Ir-C(8)	2.20(2)	Ir-C(9)	2.25(2)
S(1)-C(4)	1.79(2)	S(1)-C(5)	1.78(2)
O(1)-N(1)	1.07(3)	O(2)-C(6)	1.36(3)
C(3)-C(4)	1.54(3)	C(5)-C(6)	1.39(3)
Angles (deg)			
S(1)-Ir-S(1')	101.8(3)	S(1)-Ir-N(1)	88.8(5)
S(1)-Ir-C(8)	85.1(5)	S(1)-Ir-C(8)'	156.6(5)
S(1)-Ir-C(9)	88.1(5)	S(1)-Ir-C(9)'	163.8(5)
N(1)-Ir-C(8)	113.8(7)	N(1)-Ir-C(9)	78.4(7)
C(8)-Ir-C(8)'	81(1)	C(8)-Ir-C(9)	35.6(6)
C(8)-Ir-C(9)'	90.9(7)	C(9)-Ir-C(9)'	80(1)
Ir-N(1)-O(1)	137(2)	C(4)-S(1)-C(5)	101(1)
C(6)-O(2)-C(6)'	124(3)		

materials and produces colorless crystalline material of high purity. The ^1H NMR spectrum of ODT[9]OC shows the expected multiplet pattern for *ortho*-aromatic substitution and a single peak for the benzylic protons. The $\text{OCH}_2\text{CH}_2\text{S}$ linkage is observed as two well-separated triplets at 3.83 ppm for OCH_2 and 2.81 ppm for CH_2S . The $^{13}\text{C}\{^1\text{H}\}$ NMR spectrum of ODT[9]OC is straightforward, exhibiting three well-defined resonances for the aromatic carbons at 137.17, 130.79, and 127.59 ppm and separate resonances for the OCH_2 , benzylic, and SCH_2 carbons at 72.20, 33.97, and 32.57 ppm, respectively.

Synthesis of $[\text{M}(\text{COD})(\text{L})][\text{BF}_4]$ Complexes. Rh(I) and Ir(I) complexes of TT[9]OC and ODT[9]OC were prepared by displacing solvent from $[\text{M}(\text{COD})(\text{acetone})_2]$ -

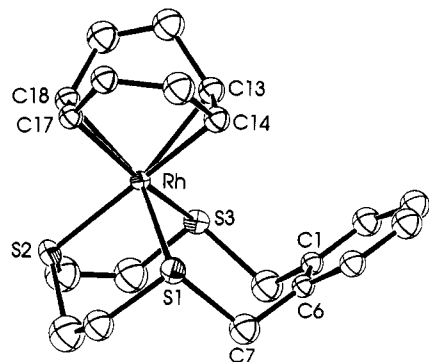
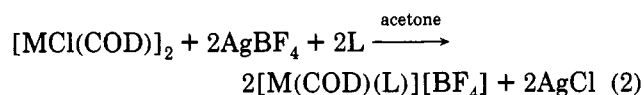


Figure 1. ORTEP drawing of the $[\text{Rh}(\text{COD})(\text{TT}[9]\text{OC})]^+$ cation of **1**, showing the atom-numbering scheme. Carbon atoms are numbered sequentially, beginning with the aromatic ring of TT[9]OC. Thermal ellipsoids of 30% probability are shown.

$[\text{BF}_4]$, which was prepared *in situ* from the reaction of $[\text{MCl}(\text{COD})]_2$ with 2 equiv of AgBF_4 in acetone as summarized in eq 2.



Yields of these complexes range from 65 to 77%, and the yellow or orange materials are soluble in polar organic solvents such as acetone and acetonitrile. ^1H NMR resonances for coordinated TT[9]OC or ODT[9]OC are consistent with a symmetrical coordination mode in which both benzylic sulfur atoms are coordinated to the metal. This could either be the expected facial coordination or an S_2 -bidentate chelation.¹⁶ The most notable NMR spectral feature is the splitting of the benzylic proton resonances from a singlet, as observed in the free ligand, to a pair of doublets upon complexation. This results from coordination of the benzylic sulfur atoms in a symmetrical fashion and formation of a seven-membered chelate ring which places the benzylic protons in axial and equatorial positions. In the Rh complexes, a small, 1–3 Hz, three-bond Rh–H coupling was also observed to the downfield doublet. These benzylic resonances are readily apparent in the ^1H NMR spectra of all four $[\text{M}(\text{COD})(\text{L})]^+$ complexes and are a useful spectroscopic tool for monitoring the extent of reaction in these systems.

X-ray Structure of $[\text{Rh}(\text{COD})(\text{TT}[9]\text{OC})][\text{BF}_4]$ (1**).** A perspective ORTEP drawing of the complex cation of **1** is shown in Figure 1. $[\text{Rh}(\text{COD})(\text{TT}[9]\text{OC})]^+$ is five-coordinate with an overall geometry best described as distorted trigonal bipyramidal. TT[9]OC is coordinated in a facial manner to two equatorial sites with relatively long Rh–S distances of Rh–S(1) = 2.422(4) Å and Rh–S(3) = 2.494(5) Å and one axial site with a shorter Rh–S distance of Rh–S(2) = 2.316(5) Å. The larger seven-membered chelate ring involving the xylyl group spans the two equatorial coordination sites with an angle of 102.0(2)° for S(1)–Rh–S(3), while the angles at Rh for the two five-membered chelate rings are 86.2(2) and 84.5(5)° for S(1)–Rh–S(2) and S(2)–Rh–S(3), respectively. The COD ligand occupies the remaining equatorial and axial sites in the trigonal bipyramid with the Rh–C distances Rh–C(13) = 2.23(2) Å and Rh–C(14) = 2.18(2) Å for the olefinic bond in the axial position being slightly longer than those in the equatorial position, Rh–C(17) = 2.12(2) Å and Rh–C(18) = 2.10(2) Å.

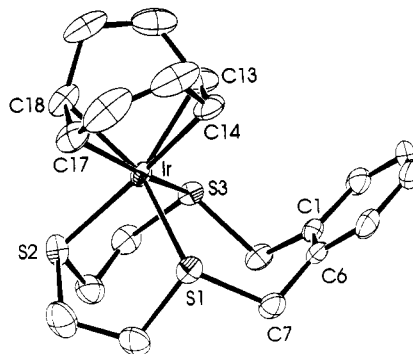


Figure 2. ORTEP drawing of the $[\text{Ir}(\text{COD})(\text{TT}[9]\text{OC})]^+$ cation of **2**, showing the atom-numbering scheme. Carbon atoms are numbered sequentially, beginning with the aromatic ring of TT[9]OC. Thermal ellipsoids of 30% probability are shown.

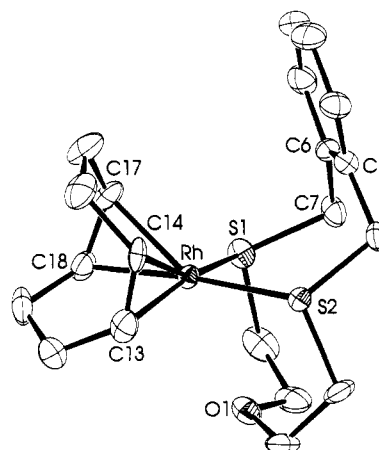


Figure 3. ORTEP drawing of the $[\text{Rh}(\text{COD})(\text{ODT}[9]\text{OC})]^+$ cation of **3**, showing the atom-numbering scheme. Carbon atoms are numbered sequentially, beginning with the aromatic ring of ODT[9]OC. Thermal ellipsoids of 30% probability are shown.

X-ray Structure of $[\text{Ir}(\text{COD})(\text{TT}[9]\text{OC})][\text{BF}_4]$ (2**).** A perspective ORTEP drawing of the complex cation of **2** is shown in Figure 2. The solid-state structure of $[\text{Ir}(\text{COD})(\text{TT}[9]\text{OC})]^+$ is similar to that of **1**, showing the same distorted trigonal bipyramidal geometry. TT[9]OC is coordinated in a facial manner to two equatorial sites and one axial site, but the variation in bond distances between these two sites is not as pronounced as for **1**; Ir–S(1) = 2.444(3) Å, Ir–S(3) = 2.375(2) Å, and Ir–S(2) = 2.317(3) Å. Also, as in **1**, the seven-membered chelate ring spans the two equatorial coordination sites with a larger angle of 100.33(8)° for S(1)–Ir–S(3), while the angles for the two five-membered chelate rings are 86.7(1) and 85.8(1)° for S(1)–Ir–S(2) and S(2)–Ir–S(3), respectively. The COD ligand occupies the remaining equatorial and axial sites in the trigonal bipyramid with Ir–C(13) = 2.17(1) Å, Ir–C(14) = 2.20(1) Å, Ir–C(17) = 2.12(1) Å, and Ir–C(18) = 2.12(1) Å.

X-ray Structure of $[\text{Rh}(\text{COD})(\text{ODT}[9]\text{OC})][\text{BF}_4]$ (3**).** A perspective ORTEP drawing of the complex cation of **3** is shown in Figure 3. $[\text{Rh}(\text{COD})(\text{ODT}[9]\text{OC})]^+$ is four-coordinate with a square planar geometry. The mixed S,O-donor ligand ODT[9]OC is coordinated to the Rh center by only the two benzylic sulfur atoms with Rh–S distances of Rh–S(1) = 2.373(3) Å and Rh–S(2) = 2.431(3) Å. Although the oxygen donor atom of ODT[9]OC is in an endodentate position required for chelation to the metal,

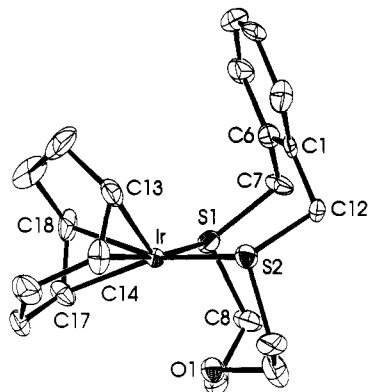


Figure 4. ORTEP drawing of the $[\text{Ir}(\text{COD})(\text{ODT}[9]\text{OC})]^+$ cation of **4**, showing the atom-numbering scheme. Carbon atoms are numbered sequentially, beginning with the aromatic ring of ODT[9]OC. Thermal ellipsoids of 30% probability are shown.

there is no Rh–O bond, as the Rh...O(1) distance is 2.717(8) Å. The angle subtended at rhodium involving the xylyl group is slightly larger than the ideal angle of 90° (S(1)–Rh–S(2) = 100.9(1)°), but this is presumably required to accommodate the large and relatively rigid seven-membered ring. The COD ligand chelates to the remaining coordination sites of the square plane with Rh–C distances of Rh–C(13) = 2.15(1) Å, Rh–C(14) = 2.19(1) Å, Rh–C(17) = 2.12(1) Å, and Rh–C(18) = 2.12(1) Å.

X-ray Structure of $[\text{Ir}(\text{COD})(\text{ODT}[9]\text{OC})][\text{BF}_4]$ (4**).** As with the solid-state structures of **1** and **2**, the structures of the Rh(I) and Ir(I) complexes containing ODT[9]OC are also similar. A perspective ORTEP drawing of the complex cation of **4** is shown in Figure 4. $[\text{Ir}(\text{COD})(\text{ODT}[9]\text{OC})]^+$ is four-coordinate with a square-planar geometry and the mixed S,O-donor ligand ODT[9]OC coordinated to Ir by the two benzylic sulfur atoms. The Ir–S distances are Ir–S(1) = 2.407(6) Å and Ir–S(2) = 2.348(5) Å with a nonbonding Ir...O(1) distance of 2.59(1) Å and chelate angle of 100.8(2)° for S(1)–Ir–S(2). The COD ligand chelates to the remaining coordination sites of the square plane with Ir–C distances of Ir–C(13) = 2.08(2) Å, Ir–C(14) = 2.02(3) Å, Ir–C(17) = 2.14(2) Å, and Ir–C(18) = 2.20(2) Å.

Reaction of $[\text{M}(\text{COD})(\text{L})][\text{BF}_4]$ with CO. The reaction chemistry of **1–4** with CO is summarized in Schemes 1–3. $[\text{Rh}(\text{COD})(\text{TT}[9]\text{OC})][\text{BF}_4]$ (**1**) and $[\text{Ir}(\text{COD})(\text{TT}[9]\text{OC})][\text{BF}_4]$ (**2**) are coordinatively saturated, 18-electron species and, as such, are relatively unreactive. Substitution reactions to replace COD with phosphine or acetylenes and reactions with H₂ did not result in the formation of isolable products containing the thioether ligand. However, stirring a concentrated solution of **1** under an atmosphere of CO for 5 min results in a color change from orange to brick red. $^{13}\text{C}\{^1\text{H}\}$ and ^1H NMR spectroscopy show the formation of two products identified as the dicarbonyl complex $[\text{Rh}(\text{CO})_2(\text{TT}[9]\text{OC})][\text{BF}_4]$ (**5**) and the binuclear carbonyl complex $[(\text{TT}[9]\text{OC})\text{Rh}(\mu\text{-CO})_3\text{Rh}(\text{TT}[9]\text{OC})][\text{BF}_4]_2$ (**6**), which contains a Rh–Rh bond. Replacing the CO(g) atmosphere with N₂(g) results in complete conversion to **6**, and orange-red microcrystals of **6** could be isolated by removing the solvent from the reaction mixture, washing the residue with diethyl ether to remove COD, and recrystallizing from a saturated solution at –10 °C. The IR spectrum of **5** shows two terminal ν_{CO} absorptions at 2059 and 1933 cm^{–1}, while **6**

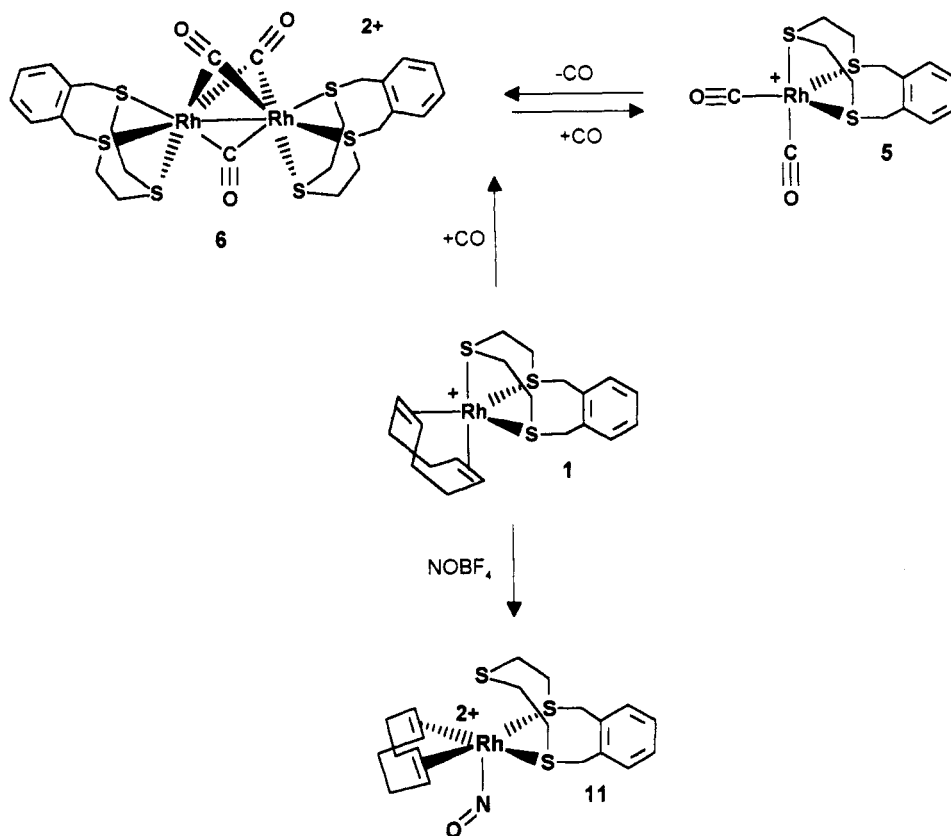
exhibited ν_{CO} absorptions at 1862 and 1841 cm^{–1}, indicative of bridging carbonyl groups.²⁵

In contrast, the analogous Ir complex $[\text{Ir}(\text{COD})(\text{TT}[9]\text{OC})][\text{BF}_4]$ (**2**) was quite inert to substitution by CO. When a solution of **2** was refluxed for an extended period of time, under an atmosphere of CO, a single product was detected by NMR spectroscopy (ca. 5%) but could not be isolated. In order to increase the likelihood of CO substitution for olefin, $[\text{IrCl}(\text{COE})_2]_2$ was reacted with AgBF₄ in a donor solvent under N₂ in the presence of TT[9]OC (presumably forming $[\text{Ir}(\text{COE})_2(\text{TT}[9]\text{OC})][\text{BF}_4]$, not isolated), followed by the introduction of an atmosphere of CO(g). The major product from this reaction was isolated and identified as $[\text{Ir}(\text{CO})(\text{COE})(\text{TT}[9]\text{OC})][\text{BF}_4]$ (**7**). The ^1H NMR spectrum of **7** shows that COE is still present in the complex, while the $^{13}\text{C}\{^1\text{H}\}$ NMR spectrum at 235 K shows only one resonance at 184 ppm due to CO, as well as peaks attributable to TT[9]OC and COE. A single ν_{CO} absorption was observed at 2073 cm^{–1} in the infrared spectrum. Another minor product from this reaction was shown to be identical with that produced from the reaction of **2** with CO but again could not be isolated in a sufficient quantity for full characterization. However, it was found that by changing the conditions for the substitution reaction employing $[\text{IrCl}(\text{COE})_2]_2$, it was possible to prepare the minor component from these previous reactions as the major product. First $[\text{IrCl}(\text{COE})_2]_2$ was reacted with AgBF₄ under an atmosphere of CO(g) to yield an intensely blue-green solid that is insoluble in CH₃CN. This was then followed by the addition of solid TT[9]OC, which after 20 min produced a yellow solution. After the solution was filtered to remove precipitate AgCl and solvent was removed, $[\text{Ir}(\text{CO})_2(\text{TT}[9]\text{OC})][\text{BF}_4]$ (**8**) was isolated in 46% yield. The ^1H NMR spectrum shows only resonances for coordinated ligand, while the low-temperature $^{13}\text{C}\{^1\text{H}\}$ NMR spectrum shows CO resonances at 175 and 168 ppm as well as the expected resonances for coordinated TT[9]OC. The infrared spectrum shows two ν_{CO} absorptions at 2095 and 2045 cm^{–1}.

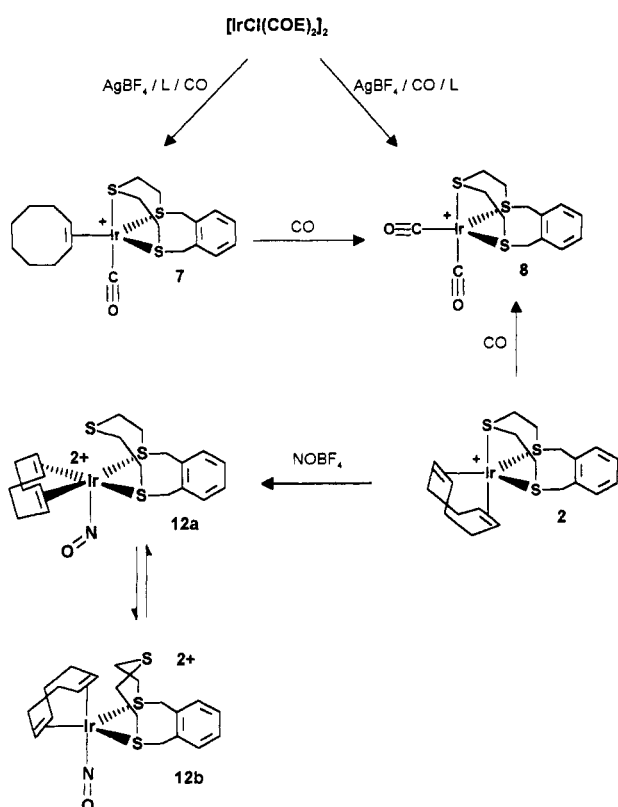
The coordinatively unsaturated complexes **3** and **4**, containing ODT[9]OC, were expected to be much more reactive than **1** and **2**, and this was certainly the case. $[\text{Rh}(\text{COD})(\text{ODT}[9]\text{OC})][\text{BF}_4]$ (**3**) reacts immediately with CO to precipitate the yellow product **9**, which is soluble in acetone and acetonitrile. The infrared spectrum of **9** shows three ν_{CO} absorptions at 2103, 2044, and 2015 cm^{–1}, consistent with the assignment of **9** as the coordinatively saturated tricarbonyl species $[\text{Rh}(\text{CO})_3(\text{ODT}[9]\text{OC})][\text{BF}_4]$, while the ^1H NMR spectrum at 210 K shows the expected resonances for a product in which only the S atoms are bound to Rh. In the reaction of $[\text{Ir}(\text{COD})(\text{ODT}[9]\text{OC})][\text{BF}_4]$ (**4**) with CO in acetone, definitive color changes are observed from orange to red-purple to pale orange followed by the precipitation of an orange solid, **10**, which is soluble in acetonitrile. The ^1H NMR spectrum of **10** is unusual since it clearly shows two sets of benzylic resonances, indicating that ODT[9]OC is asymmetrically bound to the Ir center. This asymmetry is similar to that identified in the structure of the related complex $[\text{PdCl}_2(\text{TT}[9]\text{MC})]^{15}$, in which TT[9]MC (the *meta* isomer of TT[9]OC) acts as a bidentate ligand, coordinating through only one benzylic sulfur atom and the central aliphatic

(25) Collman, J. P.; Hegedus, L. S. *Principles and Applications of Organotransition Metal Chemistry*; University Science Books: Mill Valley, CA, 1988.

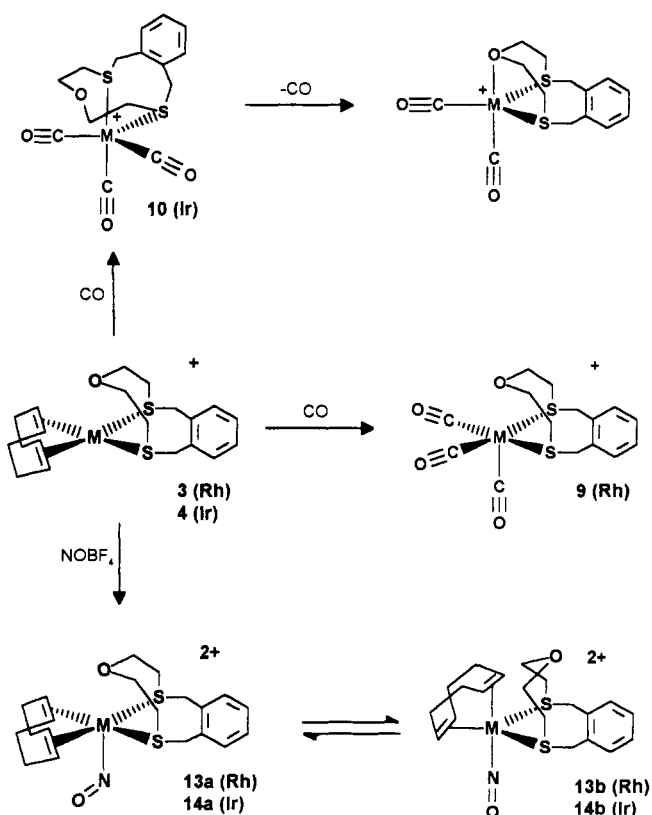
Scheme 1



Scheme 2



Scheme 3



sulfur atom to form a five-membered chelate ring. The $^{13}\text{C}\{^1\text{H}\}$ NMR spectrum of 10 is consistent with this structural assignment, since three CO resonances and separate peaks for all ligand carbon atoms are observed. The IR spectrum shows only one broad, strong ν_{CO} absorption at 2042 cm^{-1} . Cooling an acetonitrile solution

of 10 to $-20\text{ }^\circ\text{C}$ results in the precipitation of a purple product. The IR spectrum of this purple solid exhibits two absorptions at 2052 and 1968 cm^{-1} , but the ^1H NMR spectrum showed only broad resonances at the low temperatures required for generation of this complex in

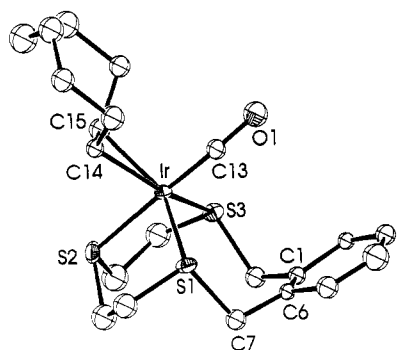


Figure 5. ORTEP drawing of the $[\text{Ir}(\text{COE})(\text{CO})(\text{TT}[9]\text{OC})]^+$ cation of **7**, showing the atom-numbering scheme. Carbon atoms are numbered sequentially, beginning with the aromatic ring of $\text{TT}[9]\text{OC}$. Thermal ellipsoids of 30% probability are shown.

solution. A possible structural assignment is the dicarbonyl complex $[\text{Ir}(\text{CO})_2(\text{ODT}[9]\text{OC})][\text{BF}_4]$, formed by coordination of the O atom and loss of CO at low temperature.

X-ray Structure of $[\text{Ir}(\text{COE})(\text{CO})(\text{TT}[9]\text{OC})][\text{BF}_4]$ (7**).** A perspective ORTEP drawing of the complex cation of **7** is shown in Figure 5. $[\text{Ir}(\text{COE})(\text{CO})(\text{TT}[9]\text{OC})]^+$ is five-coordinate with a distorted trigonal bipyramidal geometry. $\text{TT}[9]\text{OC}$ is coordinated in a facial manner to two equatorial sites with Ir–S distances Ir–S(1) = 2.39(2) Å and Ir–S(3) = 2.41(1) Å and one axial site with the Ir–S distance Ir–S(2) = 2.35(1) Å. The seven-membered chelate ring involving the xylyl group spans the two equatorial coordination sites with an angle of 106.8(4)° for S(1)–Ir–S(3), while the angles at Ir for the two five-membered chelate rings are 87.5(5) and 85.9(5)° for S(1)–Ir–S(2) and S(2)–Ir–S(3), respectively. The COE and CO ligands occupy the remaining equatorial and axial sites, respectively, with an Ir–C distance of 1.70(4) Å for the carbonyl group and distances Ir–C(14) = 2.17(5) Å and Ir–C(15) = 2.18(4) Å for the olefinic bond.

Reactions of $[\text{M}(\text{COD})(\text{L})][\text{BF}_4]$ with NOBF_4 . The reaction chemistry of **1–4** with NO^+ is summarized in Schemes 1–3. In general, the reactions of **1–4** with 1 equiv of NOBF_4 are identical, differing only in the apparent thermal stability of the adducts **11–14** formed. In each case, the ^1H NMR spectrum was recorded immediately upon mixing the two reagents. Only the adduct **14** derived from **4** was stable enough to allow isolation of a solid product. Complex **11**, $[\text{Rh}(\text{NO})(\text{COD})(\text{TT}[9]\text{OC})][\text{BF}_4]_2$, was the least stable product; at -78°C the reaction mixture immediately turned dark brown and precipitated a brown solid which was thermally unstable. ^1H NMR and solution IR spectroscopy showed evidence for only one product in solution with the presence of free COD. Similar reactions with **2–4** produced adducts **12–14**, which showed increasing stability on going from $\text{TT}[9]\text{OC}$ to $\text{ODT}[9]\text{OC}$ and from Rh(I) to Ir(I). ^1H and $^{13}\text{C}\{^1\text{H}\}$ NMR and solution IR spectra of these three NO complexes showed the presence of two products in solution, while the solid-state infrared spectrum for **14** exhibited a single ν_{NO} stretching frequency.²⁵

The observation of two species in solution for **11–14** is significant, since this occurred even when isolated X-ray-quality crystals of **14** were used for the NMR sample. Both solution complexes are symmetrical, and the results of NMR decoupling experiments and solution IR measurements suggest that the observation of two compounds is the result of an equilibrium between a square pyramidal

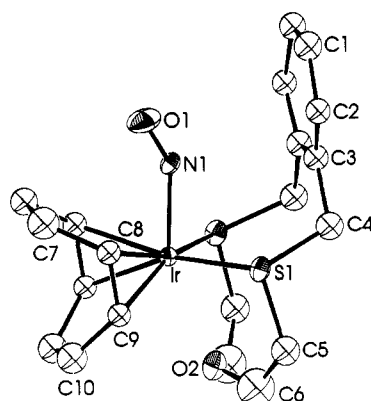


Figure 6. ORTEP drawing of the $[\text{Ir}(\text{NO})(\text{COD})(\text{ODT}[9]\text{OC})]^{2+}$ cation of **14**, showing the atom-numbering scheme. Carbon atoms are numbered sequentially, beginning with the aromatic ring of $\text{ODT}[9]\text{OC}$. Thermal ellipsoids of 30% probability are shown.

M(III) product containing a bent NO ligand (formally NO^+), as observed for the solid-state structure of **14** (vide infra), and a trigonal bipyramidal M(I) product containing a linear NO ligand (formally NO^-). This is strongly reminiscent of the complexes $[\text{CoCl}_2(\text{NO})(\text{PR}_3)_2]$ studied by Collman and Ibers.²⁶ The observation of slightly higher values of ν_{NO} for the compounds in this work (1708 cm^{-1} for **14** versus 1560 cm^{-1} for $[\text{IrCl}_2(\text{NO})(\text{PPh}_3)_2]$) is presumably related to the dipositive charge associated with these species.²⁶

The complexes **3** and **4** containing $\text{ODT}[9]\text{OC}$ have square planar geometry and as such can easily accommodate the addition of NO^+ to form a square pyramidal product. This can occur without rearrangement of the macrocycle, which translates into an increased stability for **13** and **14**. Analogous reactions of NO^+ with **1** and **2** to form **11** and **12** require the axial S(2) atom of $\text{TT}[9]\text{OC}$ to be displaced in order to accommodate the NO^+ group. Although we have previously demonstrated that this ligand conformation is possible,¹⁶ it is very likely this perturbation destabilizes complexes of this ligand relative to those of $\text{ODT}[9]\text{OC}$.

X-ray Structure of $[\text{Ir}(\text{NO})(\text{COD})(\text{ODT}[9]\text{OC})][\text{BF}_4]_2$ (14**).** A perspective ORTEP drawing of the complex cation of **14** is shown in Figure 6. The cation is situated on a crystallographic mirror plane which bisects both chelating ligands and results in a 50:50 disorder of the NO oxygen atom on each side of the mirror. Both BF_4^- anions (one displaying a 3-fold rotational disorder; 50:50) also sit on the mirror, as does a water molecule which is H-bonded between the two anions. $[\text{Ir}(\text{COD})(\text{NO})(\text{ODT}[9]\text{OC})]^{2+}$ exhibits distorted square pyramidal geometry with the mixed S,O-donor ligand $\text{ODT}[9]\text{OC}$ coordinated to Ir by the two benzylic sulfur atoms. The NO group is bent (Ir–N(1)–O(1) = 137(2)°) and occupies the apical position such that the O(1)–N(1)–O(1') angle is 67(4)°. The Ir–S distances are Ir–S(1) = 2.407(6) Å and Ir–S(2) = 2.348(5) Å with a nonbonding Ir...O(1) distance of 2.87(3) Å and a chelate angle of 100.8(2)° for S(1)–Ir–S(2). The COD ligand chelates to the remaining coordination sites of the square plane with Ir–C distances Ir–

(26) (a) Collman, J. P.; Farnham, P. H.; Dolcetti, G. *J. Am. Chem. Soc.* 1971, 93, 1789–1790. (b) Brock, C. P.; Collman, J. P.; Dolcetti, G.; Farham, P. H.; Ibers, J. A.; Lester, J. E.; Reed, C. A. *Inorg. Chem.* 1973, 12, 1304–1313.

C(13) = 2.08(2) Å, Ir-C(14) = 2.02(3) Å, Ir-C(17) = 2.14(2) Å, and Ir-C(18) = 2.20(2) Å.

Conclusions

The trithiacyclophane TT[9]OC is capable of acting as a capping ligand for the $[M(\text{COD})]^+$ fragments ($M = \text{Rh(I)}$, Ir(I)). Analogous to the Rh(I) and Ir(I) complexes $[M(9\text{S3})(\text{COD})]^+$ and $[M(9\text{S3})(\text{C}_2\text{H}_4)_2]^+$ reported by Schröder,⁵ these complexes are trigonal bipyramidal and coordinatively saturated. However, unlike the complexes of 9S3, the complexes of TT[9]OC undergo substitution of the olefinic ligand by CO, albeit slowly, to yield the carbonyl complexes $[\text{Rh}(\text{CO})_2(\text{TT}[9]\text{OC})][\text{BF}_4]_2$ (5), $[(\text{TT}[9]\text{OC})\text{Rh}(\mu\text{-CO})_3\text{Rh}(\text{TT}[9]\text{OC})][\text{BF}_4]_2$ (6), and $[\text{Ir}(\text{CO})_2(\text{TT}[9]\text{OC})][\text{BF}_4]$ (8). This is a result of the greater flexibility of TT[9]OC and reflects this ligand's previously demonstrated ability to undergo slippage to a bidentate coordination mode.¹⁶ The accessibility of a 16-electron intermediate then facilitates the observed substitution reactions. This was successfully modeled by replacing the central S atom in TT[9]OC by an ether O atom. This results in a ligand, ODT[9]OC, which acts as a bidentate S_2 chelate and yields coordinatively unsaturated, square planar complexes which undergo facile substitution of the olefin groups by CO to yield carbonyl complexes of the type $[M(\text{CO})_3(\text{ODT}[9]\text{OC})][\text{BF}_4]$. The flexibility and

slippage of TT[9]OC from a tridentate to a bidentate mode was also demonstrated by the addition of NO^+ to the four complexes $[M(\text{COD})(\text{L})][\text{BF}_4]$. Formation of the five-coordinate NO^+ adducts $[M(\text{NO})(\text{COD})(\text{L})]^{2+}$ requires a bidentate coordination mode for the thiacyclophane. This is demonstrated by the X-ray structure of $[\text{Ir}(\text{NO})(\text{COD})(\text{ODT}[9]\text{OC})]^{2+}$ and reflected in the relative stability of the four adducts.

The synthetic, spectroscopic, and structural data described herein provide a solid background for future evaluation of complexes containing thiacyclophanes as capping, ancillary ligands. The availability of rhodium(I) and iridium(I) carbonyl complexes of these thioether macrocycles will allow direct comparison to similar complexes containing cyclopentadienyl, tripodal phosphine, and pyrazolylborate ligands.

Acknowledgment. We thank the Natural Sciences and Engineering Research Council of Canada for financial support of this research.

Supplementary Material Available: Listings of crystallographic data collection parameters, positional parameters, thermal parameters, nonessential bonding parameters, and hydrogen atom parameters for 1-4, 7, and 14 (29 pages). Ordering information is given on any current masthead page.

OM9308405